Sub-100 fs mode-locked Tm:CLTGG laser

Li Wang, Weidong Chen, Zhongben Pan, Pavel Loiko, Ji Eun Bae, Fabian Rotermund, Xavier Mateos, Uwe Griebner, Valentin Petrov

Research Article | Vol. 29, No. 20 / 27 Sep 2021 / Optics Express 31137

Optics EXPRESS

Sub-100 fs mode-locked Tm:CLTGG laser

LI WANG,[1] WEIDONG CHEN,[1,2,*] ZHONGBEN PAN,[3] PAVEL LOIKO,[4] JI EUN BAE,[5] FABIAN ROTERMUND,[5] XAVIER MATEOS,[6] UWE GRIEBNER,[1] AND VALENTIN PETROV[1]

[1]*Max Born Institute for Nonlinear Optics and Short Pulse Spectroscopy, Max-Born-Str. 2a, 12489 Berlin, Germany*
[2]*Fujian Institute of Research on the Structure of Matter, Chinese Academy of Sciences, Fuzhou, 350002 Fujian, China*
[3]*Institute of Chemical Materials, China Academy of Engineering Physics, Mianyang 621900, China*
[4]*Centre de Recherche sur les Ions, les Matériaux et la Photonique (CIMAP), UMR 6252 CEA-CNRS-ENSICAEN, Université de Caen, 6 Boulevard Maréchal Juin, 14050 Caen Cedex 4, France*
[5]*Department of Physics, Korea Advanced Institute of Science and Technology (KAIST), 34141 Daejeon, Republic of Korea*
[6]*Universitat Rovira i Virgili, Física i Cristal·lografia de Materials i Nanomaterials (FiCMA-FiCNA), 43007, Tarragona, Spain*
[*]*Weidong.Chen@mbi-berlin.de*

Abstract: We report on the first sub-100 fs mode-locked laser operation of a Tm^{3+}-doped disordered calcium lithium tantalum gallium garnet (Tm:CLTGG) crystal. Soliton mode-locking was initiated and stabilized by a transmission-type single-walled carbon nanotube saturable absorber. Pulses as short as 69 fs were achieved at a central wavelength of 2010.4 nm with an average power of 28 mW at a pulse repetition rate of ~87.7 MHz. In the sub-100 fs regime, the maximum average output power amounted to 103 mW.

1. Introduction

Calcium niobium gallium disordered cubic garnets of the $Ca_3(Nb,Ga)_5O_{12}$ type or shortly CNGG, including those co-doped with univalent alkali metal cations such as Na^+(CNNGG) or Li^+ (CLNGG), when doped with trivalent rare earth ions ($RE^{3+} = Nd^{3+}$ or Yb^{3+}), feature significant inhomogeneous spectral broadening induced by their intrinsic structure disorder while preserving moderate thermal conductivity [1]. They have been proven to be excellent gain media for generation of femtosecond pulses at ~1 μm [2–7]. Recently, thulium (Tm^{3+}) doped CNGG-type disordered garnets, such as Tm:CNGG, Tm:CNNGG and Tm:CLNGG, profiting from their broad, smooth, and flat gain profiles extending well above 2 μm, have emerged as extremely suitable materials for sub-100-fs pulse generation at ~2 μm from passively mode-locked (ML) lasers [8]. The mode-locking results achieved with such crystals. are summarized in Table 1. An overview of gain media suitable for generation of sub-100 fs pulses around 2 μm can be found in the recent review paper [11].

Table 1. Sub-100 fs mode-locked thulium lasers based on disordered gallium garnets

Crystal	SA	P_{out}, mW	λ_L, nm	FWHM, nm	$\Delta\tau$, fs	PRF, MHz	Ref.
Tm:CNNGG	SWCNT	22	2018	52.8	84	89.9	[9]
Tm:CLNGG	SWCNT	54	2017	58	78	86.3	[10]
Tm:CLTGG	SWCNT	28	2010.4	67	69	87.7	This work

Abbreviations: SA – saturable absorber, Pout – average output power, FWHM – full width at half maximum, Δτ – pulse duration, PRF – pulse repetition frequency, SWCNT – single-walled carbon-nanotube

#435947 https://doi.org/10.1364/OE.435947
Journal © 2021 Received 6 Jul 2021; revised 29 Aug 2021; accepted 31 Aug 2021; published 14 Sep 2021

Alternatively, another multicomponent garnet host, namely calcium tantalum gallium garnet (abbreviated: CTGG), has been explored with Nd^{3+} or Yb^{3+} doping for ultrashort pulse generation at ~1 μm [12,13]. CTGG offers higher thermal conductivity as compared to CNGG which is attractive for power scalable laser operation [14]. Similar to CNGG, CTGG can be co-doped by univalent Li^+ cations for local charge compensation and elimination of unwanted cationic vacancies; such a crystal is known as CLTGG. The Li^+ cations further modify the multi-ligands around the active ions leading to additional inhomogeneous spectral broadening and expanding the potential for applications in ultrafast lasers [15].

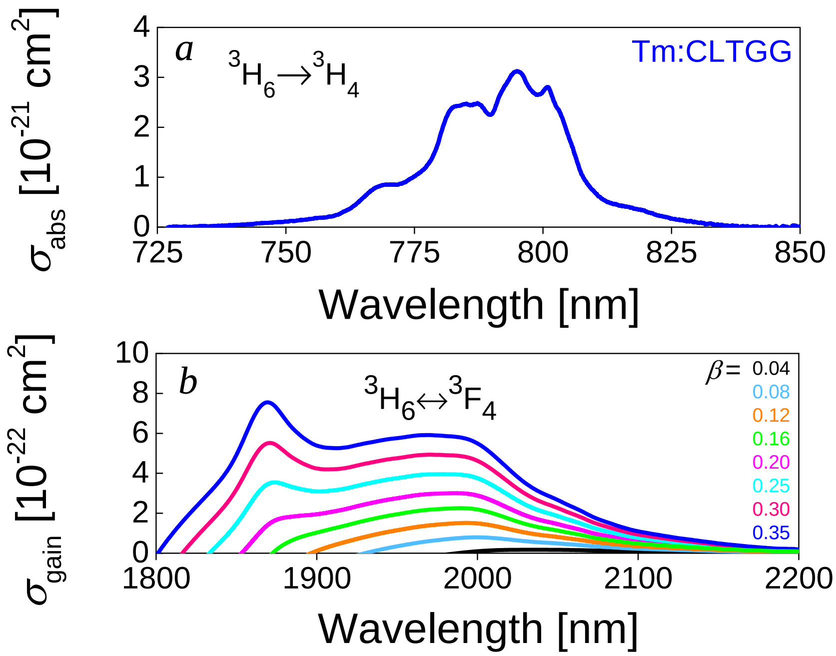

Fig. 1. Room temperature spectroscopy of the Tm:CLTGG crystal: (a) absorption cross-section, σ_{abs}, spectrum for the $^3H_6 \rightarrow ^3H_4$ transition at ~800 nm; (b) calculated gain cross-section spectra, σ_{gain}, at ~2 μm, β is the inversion ratio for Tm^{3+} ions.

Very recently, a high quality 3.17 at.% Tm^{3+}:CLTGG crystal was grown in the Institute of Chemical Materials, China Academy of Engineering Physics by the Czochralski method. It has a chemical formula of $\{Ca_{2.889}Tm_{0.093}\square_{0.018}\}[Ta_{1.32}Ga_{0.68}](Ga_{2.367}Ta_{0.204}Li_{0.345}\square_{0.084})O_{12}$, here $\square$ is the cationic vacancy. It was shown recently that Tm:CLTGG exhibits a relatively high thermal conductivity (4.33 $Wm^{-1}K^{-1}$ at room temperature [16]). The structure disorder of CLTGG results from a random distribution of Ta^{5+} and Ga^{3+} cations over octahedral and tetrahedral lattice sites. The dopant Tm^{3+} ions replace for Ca^{2+} cations. The inhomogeneous spectral broadening for the Tm^{3+} emission originates from the variation in the second coordination sphere composed by various cations (Ta^{5+}, Ga^{3+}, Li^+). The spectral broadening is observable in the absorption and emission spectra of the Tm:CLTGG crystal. The absorption cross-section, σ_{abs}, spectrum for the $^3H_6 \rightarrow ^3H_4$ transition of Tm^{3+} ions is shown in Fig. 1(a). The maximum σ_{abs} is 3.1×10^{-21} cm^2 at 795 nm. The absorption bandwidth (full width at half maximum, FWHM) is as large as 26.7 nm. This makes this new crystal attractive for pumping by high-power AlGaAs diode lasers at ~800 nm. The calculated gain cross-section, σ_{gain}, spectra for the $^3F_4 \leftrightarrow ^3H_6$ transition with different Tm inversion levels β are shown in Fig. 1(b), revealing very broad, smooth, and flat gain

Optics EXPRESS

profiles, extending up to at least 2.2 μm owing to a strong electron-phonon (vibronic) interaction [17]. The measured luminescence lifetime of the upper laser level ($^3F_4$) is 4.93 ms.

The promising spectroscopic and thermal properties of the Tm:CLTGG crystal motivated us to explore it for sub-100 fs pulse generation. In this work, we present the first soliton ML operation of a Tm:CLTGG laser delivering pulses as short as 69 fs at 2010.4 nm.

2. Experimental configuration

The continuous-wave (CW) and passively ML regimes of the Tm:CLTGG laser were investigated in an X-shaped astigmatically compensated linear cavity, as shown in Fig. 2. The uncoated crystal had an aperture of 3 mm × 3 mm and a thickness of 3.1 mm. It was mounted in a water-cooled Cu holder (coolant temperature: 12°C) and placed at Brewster's angle between two dichroic folding mirrors, M_1 and M_2, both having a radius of curvature (RoC) of -100 mm. The pump source was a narrow-linewidth CW Ti:Sapphire laser tuned to 795 nm for matching the absorption maximum. The pump beam was focused by a spherical lens (focal length, f = 70 mm) into the laser crystal resulting in a beam waist radius of 30 μm and 65 μm in the sagittal and tangential planes, respectively. The measured single-pass pump absorption under lasing conditions slightly varied as a function of the output coupling and amounted to ~40%, revealing a certain degree of ground-state bleaching. A Lyot filter (3.5-mm thick quartz plate) was inserted at Brewster's angle close to the output coupler (OC) for wavelength tuning in the CW regime.

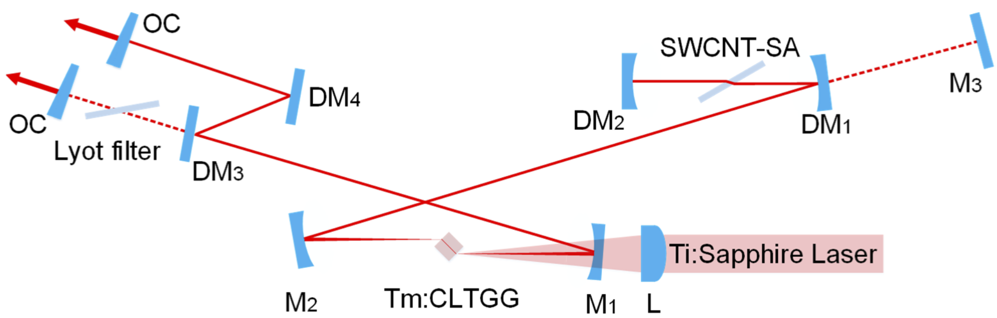

Fig. 2. Experimental arrangement of the CW and passively ML operation of Tm:CLTGG laser: L: spherical focusing lens (f = 70 mm); M_1-M_2: concave mirrors (RoC = -100 mm), M_3: flat rear mirror used in the CW regime; DM_1-DM_4, dispersive mirrors; OC: output coupler; SWCNT-SA: single-walled carbon nanotube saturable absorber.

For ML operation, a transmission-type SWCNT-SA was used to initiate and stabilize the soliton pulse shaping. The intracavity group delay dispersion (GDD) was managed by several broadband dispersive mirrors (DMs) exhibiting different negative GDD per bounce (-250 fs^2 and -125 fs^2) and more than 300 nm reflectivity bandwidth from 1850 to 2150 nm.

3. Experimental results

3.1. Continuous-wave laser operation

The performance of the CW Tm:CLTGG laser was evaluated with a four-mirror cavity including a flat rear mirror M_3 and a plane-wedged output coupler (OC) without SA, see Fig. 2. The maximum output power reached 294 mW with a 3% OC, corresponding to a slope efficiency of 26.9%, see Fig. 3(a). The laser wavelength exhibited a blue-shift with increasing OC transmission from 1995 to 1969 nm, see Fig. 3(b). The round-trip cavity loss δ and the intrinsic slope efficiency η_0 which is related to the mode matching efficiency as well as the pump quantum efficiency were estimated with the Caird analysis by fitting the measured slope efficiency as a function of the OC reflectivity, $R_{OC} = 1 - T_{OC}$ [18]. The corresponding fitting curve is shown in Fig. 3(c), giving the values of $\eta_0 = 56.7\%$ and $\delta = 0.3\%$. These values indicate a well-optimized cavity mode matching and good quality of the laser crystal. With a 0.5% OC, a broad spectral tuning range of ~286 nm (1799.4–2085.3 nm) was achieved in the CW regime at an absorbed pump power of 1.58 W, as shown in Fig. 3(d).

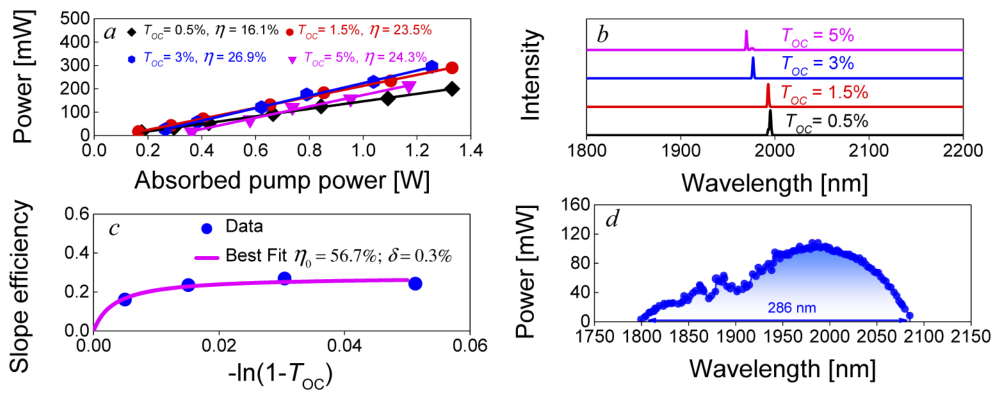

Fig. 3. Continuous-wave laser performance of the Tm:CLTGG laser: (a) input-output dependences, η – slope efficiency; (b) laser spectra; (c) evaluation of the cavity loss using the Caird approach; (d) tuning curve for a 0.5% OC in the CW regime.

3.2. Soliton mode-locked operation

For ML operation, a transmission-type SWCNT-SA was employed for initiating and stabilizing the intracavity soliton pulse shaping in the Tm:CLTGG laser. Purified SWCNTs synthesized by the dried arc-discharge method were used. The SWCNT/PMMA film was deposited on a 1-mm thick uncoated quartz substrate by spin coating [17]. The individual SWCNTs were uniformly distributed in the film and randomly oriented. The saturable absorption is due to the first fundamental transition of semiconducting carbon nanotubes (E_{11}). Due to a certain distribution of nanotube diameters (1.5–2.2 nm), the SA exhibited a broad absorption band spanning from 1.8 to 2.1 µm. The modulation depth (for normal incidence), saturation fluence, non-saturable loss and recovery time were measured at ~2 µm to be < 0.5%, ~10 µJ/cm^2, ~1% and ~1 ps, respectively [19]. The SWCNT-SA was oriented at Brewster's angle and was placed in the second beam waist created by two curved DMs, DM_1 (RoC = -100 mm, GDD = -125 fs^2) and DM_2 (RoC = -50 mm, GDD = -125 fs^2). The beam radius at the SWCNT-SA was estimated by using the ABCD matrix formalism to be 101 and 146 µm in the sagittal and tangential planes, respectively.

Initially, two additional flat DMs, DM_3 (GDD = -250 fs^2) and DM_4 (GDD = -125 fs^2), were implemented in the other cavity arm for GDD management in the ML operation. Stable and self-starting soliton mode-locking operation was obtained with a 1.5% OC and a total round-trip negative GDD of -1125 fs^2 provided by the DMs. The laser spectrum had almost perfect sech^2-shaped profile with a central wavelength of 1996 nm and emission bandwidth (FWHM) of 45 nm indicating soliton ML operation, see Fig. 4(a). The average output power amounted to 103 mW at an absorbed pump power of 1.68 W. The pulse repetition rate was ~87.7 MHz. The measured second harmonic generation (SHG) based intensity autocorrelation trace could be well fitted by a sech^2-shaped temporal pulse profile giving a pulse duration (FWHM) of 97 fs, as shown in Fig. 4(b). The corresponding time-bandwidth product (TBP) of 0.328 was only slightly above the theoretical value for sech^2-shaped pulses (0.315).

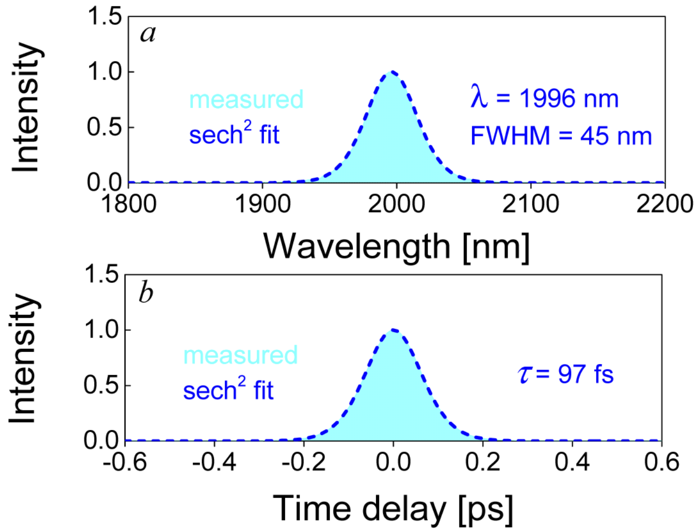

Fig. 4. (a) Spectrum of the soliton ML Tm:CLTGG laser with $T_{OC} = 1.5\%$ and (b) the corresponding SHG-based intensity autocorrelation trace.

The far-field beam profiles of the Tm:CLTGG laser for CW and soliton mode-locking regimes were measured with an IR camera (WinCamD, DataRay) placed at 1.4 m from the OC, see Fig. 5. In the CW regime, the beam profile exhibited strong interference fringes due to reflections from the front and rear surfaces of the camera neutral density filter. The measured beam diameter was 2.71 mm × 3.01 mm, as shown in Fig. 5(a). When soliton mode-locking was initiated by the SWCNT-SA, the interference fringes disappeared, see Fig. 5(b). The almost unchanged beam diameter of 2.81 mm × 3.12 mm indicates that the dominant mode-locking mechanism is soliton pulse shaping stabilized by the SWCNT-SA. The ML laser generated a nearly diffraction limited beam, as indicated by a beam quality factor (M^2) < 1.05.

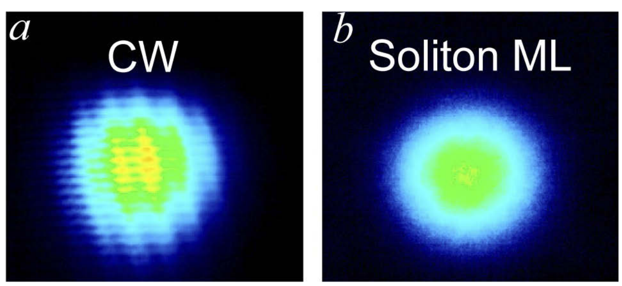

Fig. 5. Measured far-field beam profiles of the Tm:CLTGG laser ($T_{OC} = 1.5\%$): (a) CW regime; (b) soliton mode-locking regime.

The pulse duration was shortened by using lower output coupling at the expense of the average output power. An optimum performance for a 0.5% OC was achieved with all DMs having GDD = -125 fs^2, i.e., with a total round-trip GDD of -875 fs^2. The fitting of the measured spectrum and the autocorrelation trace yielded a pulse duration of 81 fs and a spectral bandwidth (FWHM) of 53.8 nm corresponding to a central wavelength of 2002.2 nm and an average power of 48 mW. The resulting TBP was 0.326, see Figs. 6(a) and 6(b).

The shortest pulse duration was obtained by using an output coupling of 0.2% OC. It was easy to achieve and stabilize mode-locking due to the cavity design ensuring strong bleaching of

Optics EXPRESS

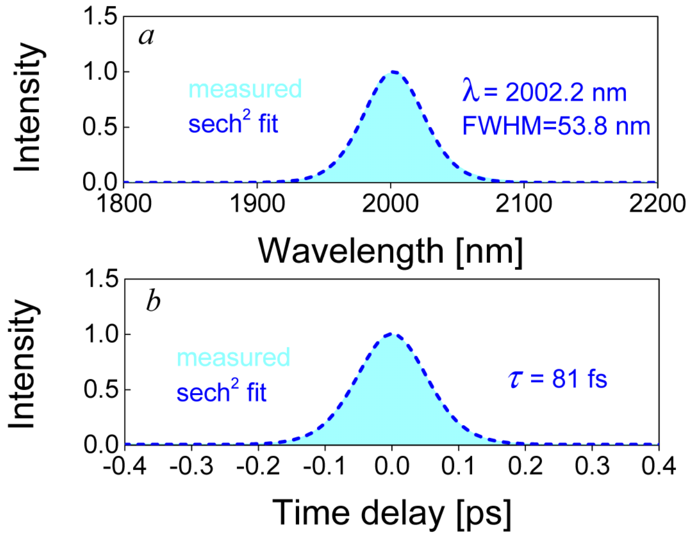

Fig. 6. (a) Optical spectrum and (b) SHG-based intensity autocorrelation trace of the soliton ML Tm:CLTGG laser for $T_{OC} = 0.5\%$.

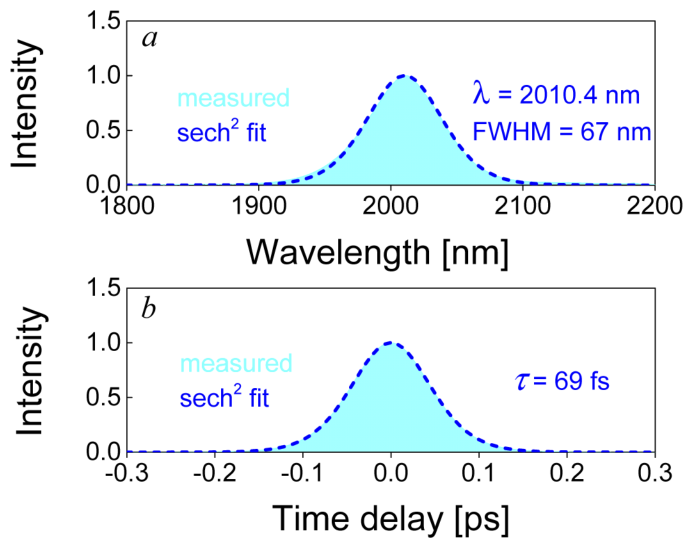

Fig. 7. (a) Optical spectrum and (b) SHG-based intensity autocorrelation trace of the soliton ML Tm:CLTGG laser for $T_{OC} = 0.2\%$.

the SA. The corresponding optical spectrum of the Tm:CLTGG laser is shown in Fig. 7(a). As expected for a quasi-three-level laser, the central wavelength experienced a further red-shift to 2010.4 nm. The spectral FWHM increased to 67 nm. Pulses as short as 69 fs were obtained after external linear chirp compensation with a 3-mm thick ZnS ceramic plate, see Fig. 7(b), for unchanged intracavity GDD management, corresponding to a TBP of 0.342. The average output power amounted to 28 mW at 87.7 MHz for an absorbed power of 1.7 W. Stable ML operation was maintained for hours without degradation of the output power and Q-switching instabilities.

The steady-state pulse train of the soliton ML Tm:CLTGG laser was characterized by a radio-frequency spectrum analyzer. A sharp peak of the fundamental beat note centered at ~87.7

MHz exhibited high signal-to-noise ratio above 70 dBc, as shown in Fig. 8(a). The latter together with the uniform harmonic beat notes seen on 1-GHz span in Fig. 8(b) indicates very stable soliton ML operation without any spurious modulation from Q-switching or multiple-pulse instabilities.

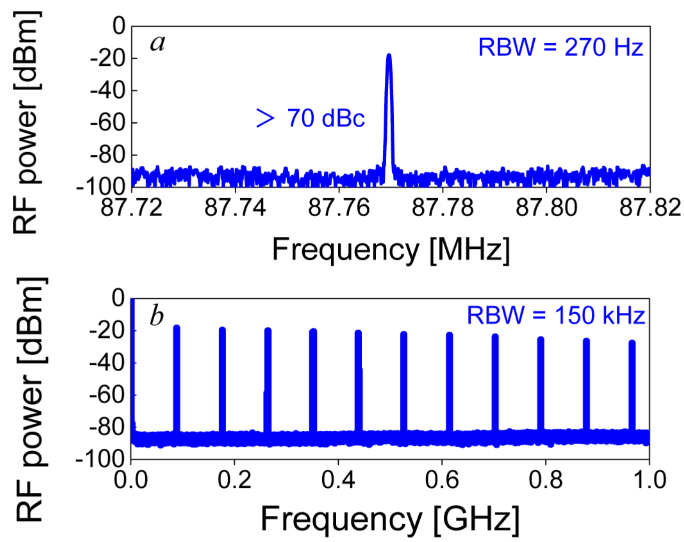

Fig. 8. Radio-frequency (RF) spectra of the soliton ML Tm:CLTGG laser: (a) fundamental beat note at ~87.7 MHz measured with a resolution bandwidth (RBW) of 270 Hz, and (b) harmonics in a 1 GHz span, measured with a RBW of 150 kHz.

4. Conclusion

In conclusion, we present a detailed investigation of a Tm:CLTGG laser in the CW regime and, for the first time, to the best of our knowledge, in the soliton mode-locked regime accessing the sub-100 fs time domain. A transmission-type SWCNT-SA was utilized for initiating and stabilizing the ML operation. Nearly transform limited soliton-like pulses as short as 69 fs were achieved at 2010.4 nm with an average output power of 28 mW and a pulse repetition rate of ~87.7 MHz. In terms of pulse duration, these results are better than the previously reported ones for ML lasers based on Tm:CNGG-type disordered garnets. As compared to these crystals, the main advantage of Tm:CLTGG is its higher thermal conductivity with weak dependence on the Tm doping, together with similar or even slightly superior inhomogeneous spectral broadening of the emission band around 2 μm. The broadband absorption and emission properties of Tm^{3+} in the disordered CLTGG crystal, the good thermal properties of this material, as well as the results of the present work, i.e., the broad tunability range and the generation of sub-100-fs pulses, indicate the potential of Tm:CLTGG for the design of ultrafast (few optical cycle) power-scalable oscillators emitting at ~2 μm, e.g., pumped by commercial high-power diode lasers at ~800 nm.

Funding. National Natural Science Foundation of China (61975208, 51761135115, 61850410533, 62075090, 52032009, 52072351); Sino-German Scientist Cooperation and Exchanges Mobility Program (M-0040); Foundation of President of China Academy of Engineering Physics (YZJJLX2018005); Key Laboratory of Optoelectronic Materials Chemistry and Physics, Chinese Academy of Sciences (2008DP173016); National Research Foundation of Korea (NRF-2020R1A4A2002828); Foundation of State Key Laboratory of Crystal Materials, Shandong University (KF2001).

Disclosures. The authors declare no conflicts of interest.

Data availability. Data underlying the results presented in this paper are not publicly available at this time but may be obtained from the authors upon reasonable request.

Optics EXPRESS

References

1. E. Castellano-Hernández, M. D. Serrano, R. J. Jimenez Rioboo, C. Cascales, C. Zaldo, A. Jezowski, and P. A. Loiko, "Na modification of lanthanide doped $Ca_3Nb_{1.5}Ga_{3.5}O_{12}$-type laser garnets: Czochralski crystal growth and characterization," Cryst. Growth Des. **16**(3), 1480–1491 (2016).
2. A. Schmidt, U. Griebner, H. Zhang, J. Wang, M. Jiang, J. Liu, and V. Petrov, "Passive mode-locking of the Yb:CNGG laser," Opt. Commun. **283**(4), 567–569 (2010).
3. Y. Zhang, V. Petrov, U. Griebner, X. Zhang, S. Y. Choi, J. Y. Gwak, F. Rotermund, X. Mateos, H. Yu, H. Zhang, and J. Liu, "90-fs diode-pumped Yb:CLNGG laser mode-locked using single-walled carbon nanotube saturable absorber," Opt. Express **22**(5), 5635–5640 (2014).
4. Y. Zhang, V. Petrov, U. Griebner, X. Zhang, H. Yu, H. Zhang, and J. Liu, "Diode-pumped SESAM mode-locked Yb:CLNGG laser," Opt. Laser Technol. **69**, 144–147 (2015).
5. J. Ma, Z. Pan, J. Wang, H. Yuan, H. Cai, G. Xie, L. Qian, D. Shen, and D. Tang, "Generation of sub-50fs soliton pulses from a mode-locked Yb,Na:CNGG disordered crystal laser," Opt. Express **25**(13), 14968–14973 (2017).
6. G. Xie, D. Tang, W. Tan, H. Luo, H. Zhang, H. Yu, and J. Wang, "Subpicosecond pulse generation from a Nd:CLNGG disordered crystal laser," Opt. Lett. **34**(1), 103–105 (2009).
7. G. Xie, L. Qian, P. Yuan, D. Tang, W. Tan, H. Yu, H. Zhang, and J. Wang, "Generation of 534 fs pulses from a passively mode-locked Nd:CLNGG-CNGG disordered crystal hybrid laser," Laser Phys. Lett. **7**(7), 483–486 (2010).
8. Z. Pan, J. M. Serres, E. Kifle, P. Loiko, H. Yuan, X. Dai, H. Cai, M. Aguiló, F. Díaz, Y. Wang, Y. Zhao, U. Griebner, V. Petrov, and X. Mateos, "Comparative study of the spectroscopic and laser properties of Tm^{3+}, $Na^+(Li^+)$-codoped $Ca_3Nb_{1.5}Ga_{3.5}O_{12}$-type disordered garnet crystals for mode-locked lasers," Opt. Mater. Express **8**(8), 2287–2299 (2018).
9. Z. Pan, Y. Wang, Y. Zhao, H. Yuan, X. Dai, H. Cai, J. E. Bae, S. Y. Choi, F. Rotermund, X. Mateos, J. M. Serres, P. Loiko, U. Griebner, and V. Petrov, "Generation of 84-fs pulses from a mode-locked Tm:CNNGG disordered garnet crystal laser," Photon. Res. **6**(8), 800–804 (2018).
10. Y. Wang, Y. Zhao, Z. Pan, J. E. Bae, S. Y. Choi, F. Rotermund, P. Loiko, J. M. Serres, X. Mateos, H. Yu, H. Zhang, M. Mero, U. Griebner, and V. Petrov, "78 fs SWCNT-SA mode-locked Tm:CLNGG disordered garnet crystal laser at 2017nm," Opt. Lett. **43**(17), 4268–4271 (2018).
11. V. Petrov, Y. Wang, W. Chen, Z. Pan, Y. Zhao, L. Wang, M. Mero, S. Y. Choi, F. Rotermund, W. B. Cho, W. Jing, H. Huang, H. Yuan, H. Cai, L. Zhang, Z. Lin, P. Loiko, X. Mateos, X. Xu, J. Xu, H. Yu, H. Zhang, S. Suomalainen, M. Guina, A. Härkönen, and U. Griebner, "Sub-100-fs bulk solid-state lasers near 2-micron," Proc. SPIE **11209**, 112094G (2019).
12. G. Xie, D. Tang, W. Tan, H. Luo, S. Guo, H. Yu, and H. Zhang, "Diode-pumped passively mode-locked Nd:CTGG disordered crystal laser," Appl. Phys. B **95**(4), 691–695 (2009).
13. F. Lou, S. Guo, J. He, B. Zhang, J. Hou, Z. Wang, X. Zhang, K. Yang, R. Wang, and X. Liu, "Diode-pumped passively mode-locked femtosecond Yb:CTGG laser," Appl. Phys. B **115**(2), 247–250 (2014).
14. C. Ma, Y. Wang, X. Cheng, M. Xue, C. Zuo, C. Gao, S. Guo, and J. He, "Spectroscopic, thermal, and laser properties of disordered garnet Nd:CLTGG crystal," J. Cryst. Growth **504**, 44–50 (2018).
15. J. Xu, S. Guo, J. He, B. Zhang, Y. Yang, H. Yang, and S. Liu, "Dual-wavelength asynchronous and synchronous mode-locking operation by a Nd:CLTGG disordered crystal," Appl. Phys. B **107**(1), 53–58 (2012).
16. A. Alles, Z. Pan, P. Loiko, J. M. Serres, S. Slimi, S. Yingming, K. Tang, Y. Wang, Y. Zhao, E. Dunina, A. Kornienko, P. Camy, W. Chen, L. Wang, U. Griebner, V. Petrov, R. M. Solé, M. Aguiló, F. Díaz, and X. Mateos, "Tm^{3+}-doped calcium lithium tantalum gallium garnet (Tm:CLTGG): novel laser crystal," Opt. Mater. Express **11**(9), 2938–2951 (2021).
17. P. Loiko, X. Mateos, S. Y. Choi, F. Rotermund, J. M. Serres, M. Aguiló, F. Díaz, K. Yumashev, U. Griebner, and V. Petrov, "Vibronic thulium laser at 2131 nm Q-switched by single-walled carbon nanotubes," J. Opt. Soc. Am. B **33**(11), D19–D27 (2016).
18. J. A. Caird, S. A. Payne, P. Staber, A. Ramponi, L. Chase, and W. F. Krupke, "Quantum electronic-properties of the $Na_3Ga_2Li_3F_{12}$:Cr^{3+} laser," IEEE J. Quantum Electron. **24**(6), 1077–1099 (1988).
19. W. B. Cho, J. H. Yim, S. Y. Choi, S. Lee, A. Schmidt, G. Steinmeyer, U. Griebner, V. Petrov, D. I. Yeom, K. Kim, and F. Rotermund, "Boosting the nonlinear optical response of carbon nanotube saturable absorbers for broadband mode-locking of bulk lasers," Adv. Funct. Mater. **20**(12), 1937–1943 (2010).